Isı Bilimi ve Tekniği Dergisi, 33, 1, 139-154, 2013
J. of Thermal Science and Technology

ISSN 1300-3615

NATURAL CONVECTION HEAT TRANSFER OF NANOFLUIDS IN A PARTIALLY DIVIDED ENCLOSURE

Semiha ÖZTUNA and Kamil KAHVECİ
Trakya University, Mechanical Engineering Department, 22180 Edirne, Turkey
tel : + 90 284 2261217, semihae@trakya.edu.tr, kamilk@trakya.edu.tr

(Geliş Tarihi: 16. 05. 2011, Kabul Tarihi: 04. 01. 2012)

Abstract: In this study, natural convection heat transfer of water-based nanofluids in a partially divided enclosure is investigated. Governing equations are solved for partition locations of 0.2, 0.4, 0.6, and 0.8, partition lengths of 0.25, 0.50, 0.75 and 1, solid volume fractions ranging from 0-10%, and Rayleigh numbers varying from 10^4 to 10^6. Three different nanoparticles, Cu, CuO, and Al_2O_3, are taken into consideration, and the ratio of the nanolayer thickness to the original particle radius is taken at a fixed value of 0.1. The results show that heat transfer decreases considerably with increasing partition height. Furthermore, as the distance of the partition from the hot wall increases, an initial decrease and subsequent increase is observed in the average Nusselt number for low Rayleigh numbers, and an initial increase and subsequent decrease is observed for high Rayleigh numbers. The results also reveal that heat transfer increases considerably when nanoparticles are used and that the largest and smallest increase are obtained for Cu and Al_2O_3 nanoparticles, respectively. Nanoparticle usage results in an increase in the average Nusselt number up to 35% for $Ra=10^4$, up to 32% for $Ra=10^5$, and up to 25% for $Ra=10^6$. The results also indicate that the average Nusselt number increases almost linearly with solid volume fraction.
Keywords: Natural convection, Nanofluid, Enclosure, PDQ, Vorticity, Stream function.

NANOAKIŞKAN İÇEREN KISMİ BÖLMELİ BİR KAPALI ORTAMDA DOĞAL KONVEKSİYONLA ISI TRANSFERİ

Özet: Bu çalışmada kısmi bölmeli bir kapalı ortamda su-bazlı nanoakışkanların doğal konveksiyonla ısı transferi incelenmiştir. Yönetici denklemler bölme yerinin 0.2, 0.4, 0.6 ve 0.8 değerleri, bölme uzunluğunun 0.25, 0.50, 0.75 ve 1 değerleri, katı hacim fraksiyonunun %0 ile %10 arasındaki değerleri ve Rayleigh sayısının 10^4 ile 10^6 arasındaki değerleri için çözülmüştür. Üç farklı nanopartikül Cu, CuO ve Al_2O_3 göz önüne alınmıştır. Nanotabaka kalınlığının orjinal parçacık yarıçapına oranı 0.1 olarak alınmıştır. Sonuçlar ısı transferinin artan bölme uzunluğu ile önemli mertebelerde düştüğünü göstermektedir. Ayrıca, bölme sıcak duvardan uzaklaştıkça küçük Rayleigh sayıları için ortalama Nusselt sayısında önce bir azalma sonra bir artış; büyük Rayleigh sayıları için ise önce bir artış sonra bir azalma gözlemlenmektedir. Sonuçlar ayrıca nanopartikül kullanımının ısı transferini önemli miktarlarda arttırdığını göstermektedir. En büyük artış Cu anoppartikül n en küçük artış ise Al_2O_3 nanopartikül için söz konusu olmaktadır. Nanopartikü kullanımı $Ra=10^4$ için %35e, $Ra=10^5$ için %32ye, $Ra=10^6$ için %25e kadar artışlara sebep olmaktadır. Sonular ayrıca ortalama Nusselt sayısının katı hacim fraksiyonu ile lineeer arttığını göstermektedir.
Anahtar Kelimeler: Doğal konveksiyon, Nanoakışkan, Kapalı ortam, PDQ, Girdap, Akım fonksiyonu.

NOMENCLATURE

a	first-order weighting coefficient
b	second-order weighting coefficient
C_p	specific heat at constant pressure
g	gravitational acceleration
H	height of the enclosure
h	height of the partition
k	thermal conductivity
L	dimensionless height of the enclosure
Nu	Nusselt number [$= h_T W/k$]
p	pressure
Pr	Prandtl number [$= \nu_f / \alpha_f$]
R	residue
Ra	Rayleigh number [$= g\beta_{T,f} W^3 \Delta T^* / (\nu_f \alpha_f)$]
T	temperature
u	velocity component in the x direction
v	velocity component in the y direction
W	width of the enclosure
x	cartesian coordinate
y	cartesian coordinate

Greek symbols

α	thermal diffusivity
β	the ratio of the nanolayer thickness
β_T	thermal expansion coefficient
ν	kinematic viscosity
η	outward variable normal to the surface
φ	solid volume fraction

μ dynamic viscosity
ρ density
ψ stream function
ω vorticity

Subscripts
a average
C cold
eff effective
f fluid
H hot
o reference value
p partition
s solid

Superscripts
* dimensional variable

INTRODUCTION

Buoyancy-driven fluid flow and heat transfer in enclosures have received considerable attention due to numerous potential engineering applications such as energy transfer in buildings, cooling of electronic devices and solar collectors. Conventional heat transfer fluids have been used as working fluids in most of previous studies that were performed in parallel with related applications (Frederic and Berbakow, 2002; Rahman and Sharif, 2003; Kahveci, 2007a-c; Kahveci and Öztuna, 2008 and 2009). However, conventional heat transfer fluids have lower thermal conductivity coefficients, which is the basic limitation of the heat transfer performance of the system considered. Recent studies have shown that this limitation, which is due to the lower thermal conductivity coefficient of conventional heat transfer fluids, can be overcome with the use of nanofluids. The term nanofluid is used to describe a solid and liquid mixture that consists of a base liquid and nanoparticles of less than 100 nm in size. Studies show that an anomalous increase is seen in thermal conductivity with the usage of nanoparticles (Eastman et al., 2001; Choi et al., 2001; Xuan and Li, 2000). Keblinski et al. (Keblinski et al., 2002) examined four possible mechanisms that could lead to this unexpected behavior. These mechanisms are: Brownian motion of nanoparticles, molecular level layering of the liquid at the liquid-particle interface, the nature of heat transfer in the nanoparticles, and nanoparticle clustering. Keblinski et al. (Keblinski et al., 2002) have also shown that Brownian motion has no significant effect on conduction while the liquid layering around nanoparticles has a fast.

There are many studies in the literature investigating the effects of nanoparticle usage on convection heat transfer. Xuan and Li (Xuan and Li, 2000) observed that oxide nanoparticles enhance heat transfer reasonably well, but metal nanoparticles have no significant effect. Eastman et al. (Eastman et al., 1998) showed that the convection heat transfer rate increases by more than 15% in water with a volume fraction of CuO of less than 1%. Wen and Ding (Wen and Ding, 2004) examined laminar flow at the entrance region of a tube through which nanofluid-containing alumina-water flowed with a 1.6% solid volume fraction; the local heat transfer coefficient at the entrance region was 41% higher than that of the base fluid with the same flow rate. Maiga et al. (Maiga et al., 2004) studied laminar and turbulent flow of nanofluids in a uniformly heated tube using approximated correlations and found that heat transfer enhancement due to nanoparticle usage becomes more important for the turbulent flow regime with increasing Reynolds numbers. Akbarinia and Behzadmehr (Akbarinia and Behzadmehr , 2007) studied laminar mixed convection of an Al_2O_3-based nanofluid in a horizontal curved tube and found that for a given nanoparticle concentration, increasing the buoyancy forces causes a reduction in skin friction. Izadi et al. (Izadi et al., 2009) performed a numerical investigation on the laminar forced convection of an Al_2O_3 and water nanofluid in an annulus and observed that the axial velocity profile does not significantly change with nanoparticle volume fraction; the temperature profiles, however, are affected by the nanoparticle concentration. Khanafer et al. (Khanafer et al., 2003) studied the natural convection of copper-based nanofluids in a differentially heated square cavity. Their results show that the presence of nanoparticles enhances heat transfer by approximately 25% for $Gr=10^4$ and $Gr=10^5$ at a volume fraction of $\varphi=0.2$. Hwang et al. (Hwang et al., 2007) studied the buoyancy-driven heat transfer of water-based Al_2O_3 nanofluids in a rectangular cavity and found that the ratio of the heat transfer coefficient of nanofluids to that of the base fluid decreases with increasing nanoparticle size. Jou and Tzeng (Jou and Tzeng, 2006) studied convective heat transfer of a copper-based nanofluid in a two-dimensional enclosure and observed that the average Nusselt number at the hot wall exhibits an increasing trend with a decrease in the aspect ratio. Oztop and Abu-Nada (Oztop and Abu-Nada, 2008) studied the natural convection of nanofluids in a partially heated enclosure and found that the increase in heat transfer is more pronounced at low aspect ratios than at high aspect ratios. Aminossadati and Ghasemi (Aminossadati and Ghasemi, 2009) investigated the natural convection cooling of a heat source embedded on the bottom wall of an enclosure filled with nanofluids and found that the type of nanoparticle and the length and location of the heat source significantly affects the maximum temperature of the heat source. Heat transfer augmentation in a two-sided, lid-driven, differentially heated square cavity utilizing nanofluids was studied numerically by Tiwari and Das (Tiwari and Das, 2007). They observed that when both vertical walls move upward in the same direction, heat transfer is reduced. They also found that when vertical walls move in the opposite directions, heat transfer is considerably enhanced for a forced convection-dominated regime. The buoyancy-driven heat transfer of water-based nanofluids in a differentially heated tilted enclosure was investigated by Kahveci (Kahveci, 2010). He found that the average heat transfer rate increases up to 44% for $Ra=10^4$, up to 53% for $Ra=10^5$, and up to 54% for $Ra=10^6$ in the special case of $\theta=90°$, which also produces the lowest heat transfer rates, is not taken into consideration. He also found that the maximum heat transfer takes place at $\theta=45°$ for $Ra=10^4$ and at $\theta=30°$ for $Ra=10^5$ and 10^6.

Convective heat transfer of nanofluids in a rectangular enclosure has been studied extensively in the literature. But the problem of convective heat transfer of nanofluids in a partitioned enclosure has not been analyzed yet. In this study, natural convection heat transfer of water-based nanofluids in a partially divided enclosure is investigated numerically and the effects of partition position and length, nanoparticle volume fraction and Rayleigh number on heat transfer are revealed.

Polynomial-Based Differential Quadrature Method

In the PDQ method (Shu, 1992; Shu, 2000; Shu and Richards, 1992; Belman et al., 1972), first and second order derivatives of f(x) at a point xi are assumed to be approximated by

$$f_x(x_i) = \sum_{j=0}^{n} a_{ij} f(x_j) \quad \text{, for } i=0,1,2,\ldots n, \tag{1}$$

$$f_{xx}(x_i) = \sum_{j=0}^{n} b_{ij} f(x_j) \quad \text{,for } i=0,1,2,\ldots.n, \tag{2}$$

where n is the number of the grid points, a_{ij} and b_{ij} are the first and second order weighting coefficients respectively. Shu and Richards (Shu and Richards, 1992) derived the following explicit formulations to compute the weighting coefficients.

$$a_{ij} = \frac{M^{(1)}(x_i)}{\left(x_i - x_j\right)M^{(1)}(x_j)} \quad j \neq i, \quad a_{ii} = -\sum_{k=1,k\neq i}^{n} a_{ik} \tag{3}$$

$$b_{ij} = 2a_{ij}\left(a_{ii} - \frac{1}{x_i - x_j}\right) \quad j \neq i, \quad b_{ii} = -\sum_{k=1,k\neq i}^{n} b_{ik} \tag{4}$$

$$M^{(1)}(x_i) = \prod_{k=1,k\neq i}^{N}\left(x_i - x_k\right) \ , \tag{5}$$

There is a recurrence relationship to compute weighting coefficients of the higher order derivatives (Belman et al., 1972). When the coordinates of grid points are known, the weighting coefficients for the discretization of derivatives can be easily calculated from equations (3-5).

ANALYSIS

The schematic of the system with coordinates is shown in Fig. 1. The square enclosure contains a vertical partition of height h.

In order to nondimensionalize the governing equations; the following dimensionless variables are used:

$$x = \frac{x^*}{W},\ y = \frac{y^*}{W},\ x_p = \frac{x_p^*}{W},\ L = \frac{H}{W},\ u = \frac{u^*}{\alpha_f / W},$$
$$v = \frac{v^*}{\alpha_f / W},\quad p = \frac{W^2}{\rho_{fo}\alpha_f^2} p^*,\ T = \frac{T^* - T_C}{T_H - T_C} \tag{6}$$

where W is the width of the enclosure, u^* and v^* are the dimensional velocity components, p^* is the dimensional pressure, T^* is the dimensional temperature, ρ_f is the fluid density, and α is the thermal diffusivity of the fluid.

For computational purposes, the domain considered in this work is divided into four regions as shown in Figure 1. The flow is assumed to be Newtonian, two-dimensional, steady and incompressible. The dimensionless governing equations can be written as follows in the vorticity-stream function formulation, after invoking the Boussinesq approximation and neglecting viscous dissipation and thermal radiation:

$$\frac{\partial^2 \psi}{\partial x^2} + \frac{\partial^2 \psi}{\partial y^2} = -\omega \tag{7}$$

$$u\frac{\partial \omega}{\partial x} + v\frac{\partial \omega}{\partial y} = \frac{\nu_{eff}}{\nu_f} Pr\left(\frac{\partial^2 \omega}{\partial x^2} + \frac{\partial^2 \omega}{\partial y^2}\right) + \frac{(\rho\beta_T)_{eff}}{\rho_{eff}\beta_{T,f}} Ra\, Pr \frac{\partial T}{\partial x} \tag{8}$$

$$u\frac{\partial T}{\partial x} + v\frac{\partial T}{\partial y} = \frac{\alpha_{eff}}{\alpha_f}\left[\frac{\partial^2 T}{\partial x^2} + \frac{\partial^2 T}{\partial y^2}\right] \tag{9}$$

Here the Prandtl and Rayleigh numbers are defined as:

$$Pr = \frac{\nu_f}{\alpha_f} \quad , \quad Ra = \frac{g\beta_{T,f} W^3 \Delta T^*}{\nu_f \alpha_f} \tag{10}$$

where ν is the kinematic viscosity of the fluid, g is the gravitational acceleration and β_T is the coefficient of thermal expansion. ΔT^* is the temperature difference between the isothermal walls of the enclosure.

The dimensionless stream function and vorticity are defined as follows:

$$u = \frac{\partial \psi}{\partial y} \quad , \quad v = -\frac{\partial \psi}{\partial x} \quad , \quad \omega = \frac{\partial v}{\partial x} - \frac{\partial u}{\partial y} \tag{11}$$

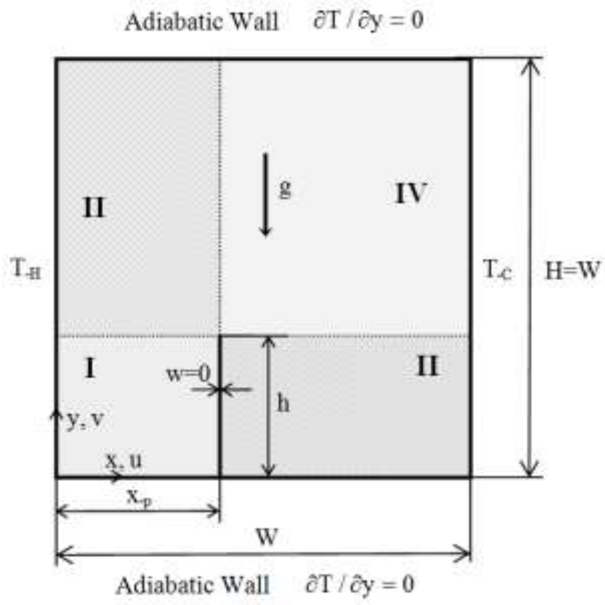

Figure 1. Geometry and coordinate system.

For the effective thermal conductivity, which is the most important thermophysical property, the following approach proposed by Yu and Choi (Yu and Choi, 2003) is used.

$$k_{eff} / k_f = \frac{k_s + 2k_f + 2(k_s - k_f)(1+\beta)^3 \varphi}{k_s + 2k_f - (k_s - k_f)(1+\beta)^3 \varphi} \qquad (12)$$

where β is the ratio of the nanolayer thickness to the original particle radius. Yu and Choi (Yu and Choi, 2003) compared their results for β=0.1 with existing experimental results from previous studies and obtained reasonably good agreement.

Nanofluid viscosity is generally estimated using existing relations for a two-phased mixture. The following Brinkman model (Brinkman, 1952) was used as the relation for the effective viscosity in this study.

$$\mu_{eff} = \mu_f / (1-\varphi)^{2.5} \qquad (13)$$

Xuan and Li (Xuan and Li, 1999) experimentally measured the effective viscosity of a transformer oil–water nanofluid and a water–copper nanofluid within a temperature range of 20–50°C. Their experimental results showed reasonably good agreement with Brinkman's theory.

Other effective properties that are present in the governing equations can be defined by the following relations.

$$(\rho C_p)_{eff} = (1-\varphi)(\rho C_p)_f + \varphi(\rho C_p)_s \qquad (14)$$

$$(\rho \beta_T)_{eff} = (1-\varphi)(\rho \beta_T)_f + \varphi(\rho \beta_T)_s \qquad (15)$$

Where

$$\rho_{eff} = (1-\varphi)\rho_f + \varphi \rho_s \qquad (16)$$

The appropriate boundary conditions for the governing equations are as follows.

$$\psi(x,0) = 0\,,\ \left.\frac{\partial T}{\partial y}\right|_{x,0} = 0\,,\ \psi(x,1) = 0\,,\ \left.\frac{\partial T}{\partial y}\right|_{x,1} = 0 \qquad (17)$$

$$\psi(0,y) = 0\,, T(0,y) = 1\,, \psi(1,y) = 0\,,$$

$$T(1,y) = 0 \qquad (18)$$

$$\psi(x_p, y) = 0\,, \quad T(x_p^-, y) = T(x_p^+, y)\,,$$

$$\left.\frac{\partial T}{\partial x}\right|_{x_p^-, y} = \left.\frac{\partial T}{\partial x}\right|_{x_p^+, y} \qquad 0 \le y \le L \qquad (19)$$

There is no physical boundary condition for the vorticity. However, an expression can be derived from a Taylor series expansion of the stream function equation as $\omega_{wall} = -\partial^2 \psi / \partial \eta^2$. Here, η is the outward direction normal to the surface. The equation above was therefore used as the boundary condition for the vorticity on the partition surfaces as well as for the enclosure surfaces in the present study.

The variation of the Nusselt number can be expressed as follows:

$$Nu = -\frac{k_{eff}}{k_f} \left.\frac{\partial T}{\partial \eta}\right|_{\eta=0} \qquad (20)$$

RESULTS AND DISCUSSION

The PDQ method [25-28], with the following non-uniform Chebyshev-Gauss-Lobatto grid point distribution, was used to transform the governing equations into a set of algebraic equations.

$$x_i = \frac{1}{2}\left[1 - \cos\left(\frac{i}{n_x}\pi\right)\right],\ i = 0,1,2,..,n_x$$

$$y_j = \frac{1}{2}\left[1 - \cos\left(\frac{j}{n_y}\pi\right)\right],\ j = 0,1,2,..,n_y \qquad (21)$$

The points in this grid system are more closely spaced in regions near the walls, where large velocity and temperature gradients are expected to develop.

The solutions of the governing equations are obtained by the successive over-relaxation (SOR) iteration method for Rayleigh numbers from 10^4 to 10^6, for partition locations ranging from 0.2 to 0.8, for partition lengths up to 1, and for solid volume fractions ranging from 0% to 10%. Three different nanoparticles (Cu, CuO, and Al_2O_3) were considered, and the ratio of the nanolayer thickness to the original particle radius was taken as a fixed value of 0.1. Water was used as the base fluid. The thermophysical properties of the fluid and solid phases are shown in Table 1. The convergence criteria were chosen as $\left|R\right|_{max} \leq 10^{-5}$, where $\left|R\right|_{max}$ is the maximum absolute residual value for the vorticity, stream function and temperature equations.

Table 1. Thermophysical properties of base fluid and nanoparticles.

Property	**Water**	**Cu**	**CuO**	**Al_2O_3**
ρ (kg/m^3)	997.1	8933	6500	3970
C_p (J/kgK)	4179	385	535.6	765
k (W/mK)	0.613	400	20	40
αx10^7 (m^2/s)	1.47	1163.1	57.45	131.7
β_Tx10^6 (1/K)	210	51	51	24

Table 2. Mesh point numbers for each region taken into consideration.

x_p	**L**		**I**	**II**	**III**	**IV**
0.2	0.25	N_x	11	11	20	20
		N_y	11	20	11	20
	0.50	N_y	15	16	15	16
	0.75	N_y	20	11	20	11
	1.00	N_y	31	-	31	-
0.4		N_x	14	17	14	17
0.6		N_x	17	14	17	14
0.8		N_x	20	11	20	11

Table 3. Grid dependency (Ra=10^6, φ=0.10, CuO).

x_p	**L**		**19x19**	**23x23**	**27x27**	**31x31**
0.2	0.25	Nu_a	10.47	10.50	10.47	10.46
		$\lvert\psi\rvert_{max}$	24.3	24.5	24.3	24.3
	0.75	Nu_a	6.43	6.53	6.44	6.43
		$\lvert\psi\rvert_{max}$	14.0	13.5	13.6	13.6
0.4	0.25	Nu_a	10.67	10.71	10.72	10.71
		$\lvert\psi\rvert_{max}$	26.4	26.6	26.5	26.5
	0.75	Nu_a	6.93	6.87	6.81	6.80
		$\lvert\psi\rvert_{max}$	22.5	22.7	22.3	22.3

Table 4. Validation of the numerical code.

	Ra=10^4		Ra=10^5		Ra=10^6	
	de Vahl Davis	Present	de Vahl Davis	Present	de Vahl Davis	Present
$\lvert\psi\rvert_{max}$	-	5.07	9.61	9.60	16.75	16.72
Nu_a	2.24	2.24	4.52	4.52	8.80	8.82
Nu_{max}	3.53	3.53	7.72	7.70	17.93	17.56
Nu_{min}	0.59	0.59	0.73	0.73	0.99	0.98

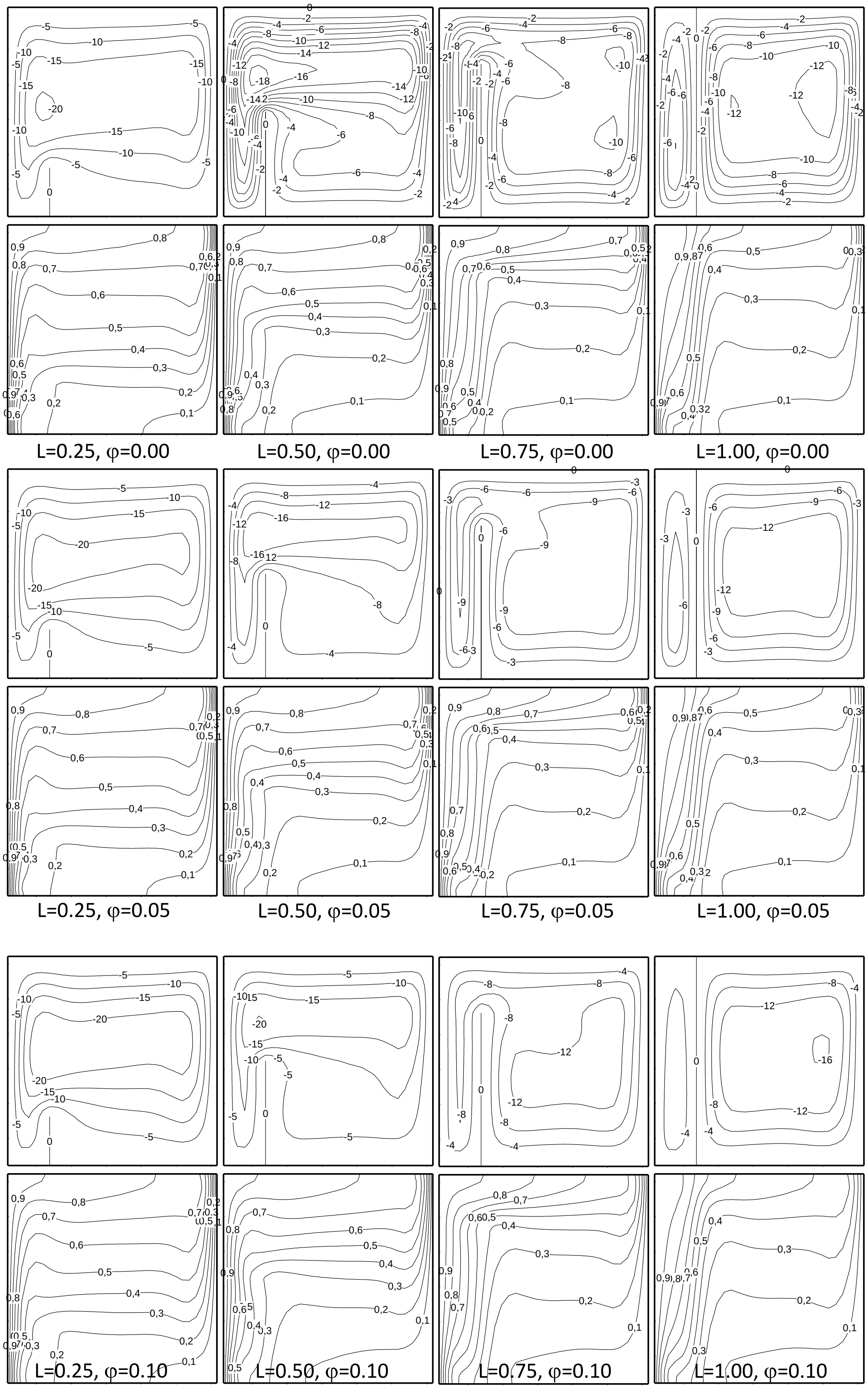

Figure 2. Streamlines and isotherms of copper based nanofluid for x_p=0.2 and Ra=10^6.

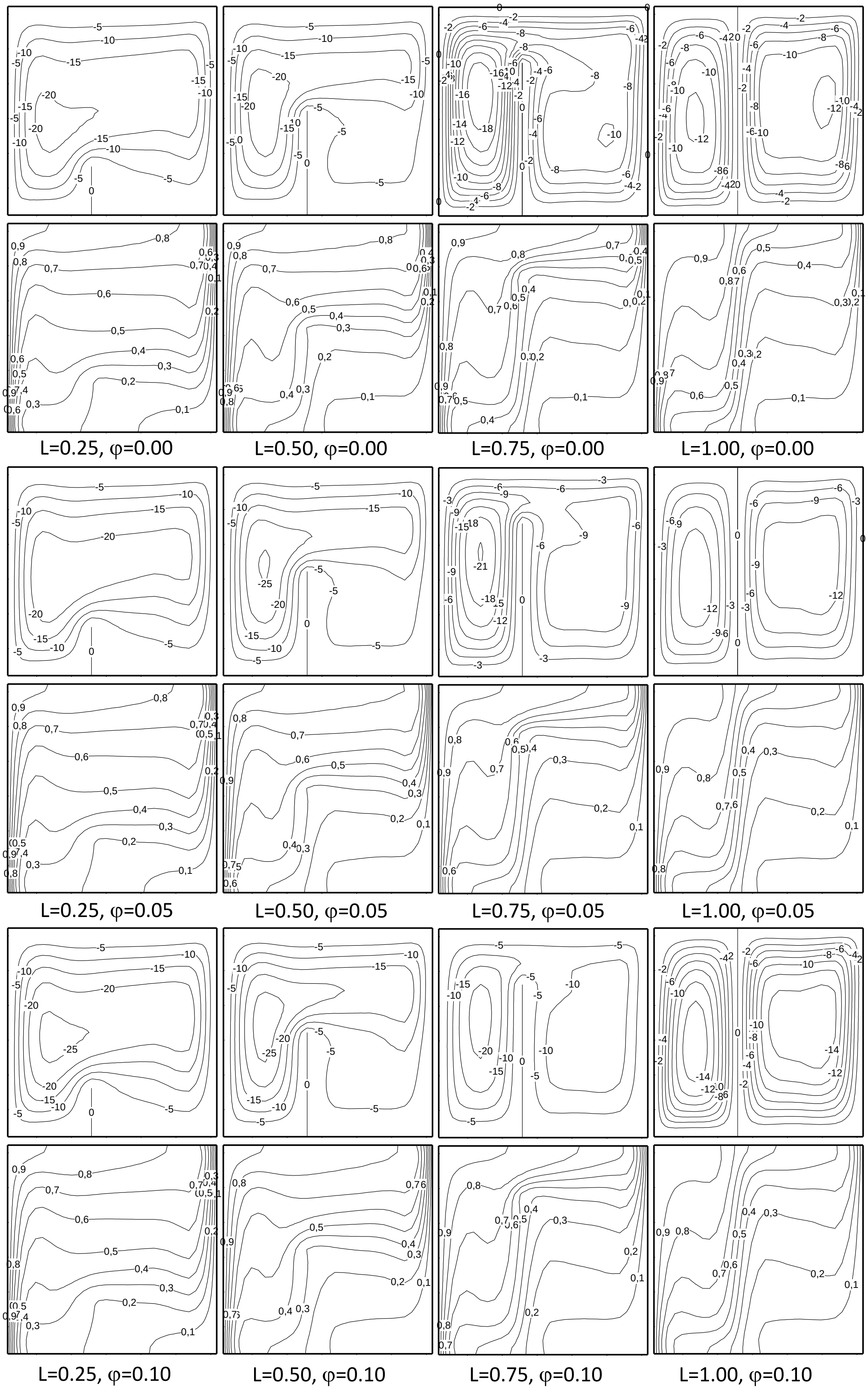

Figure 3. Streamlines and isotherms of copper based nanofluid for x_p=0.4 and Ra=10^6.

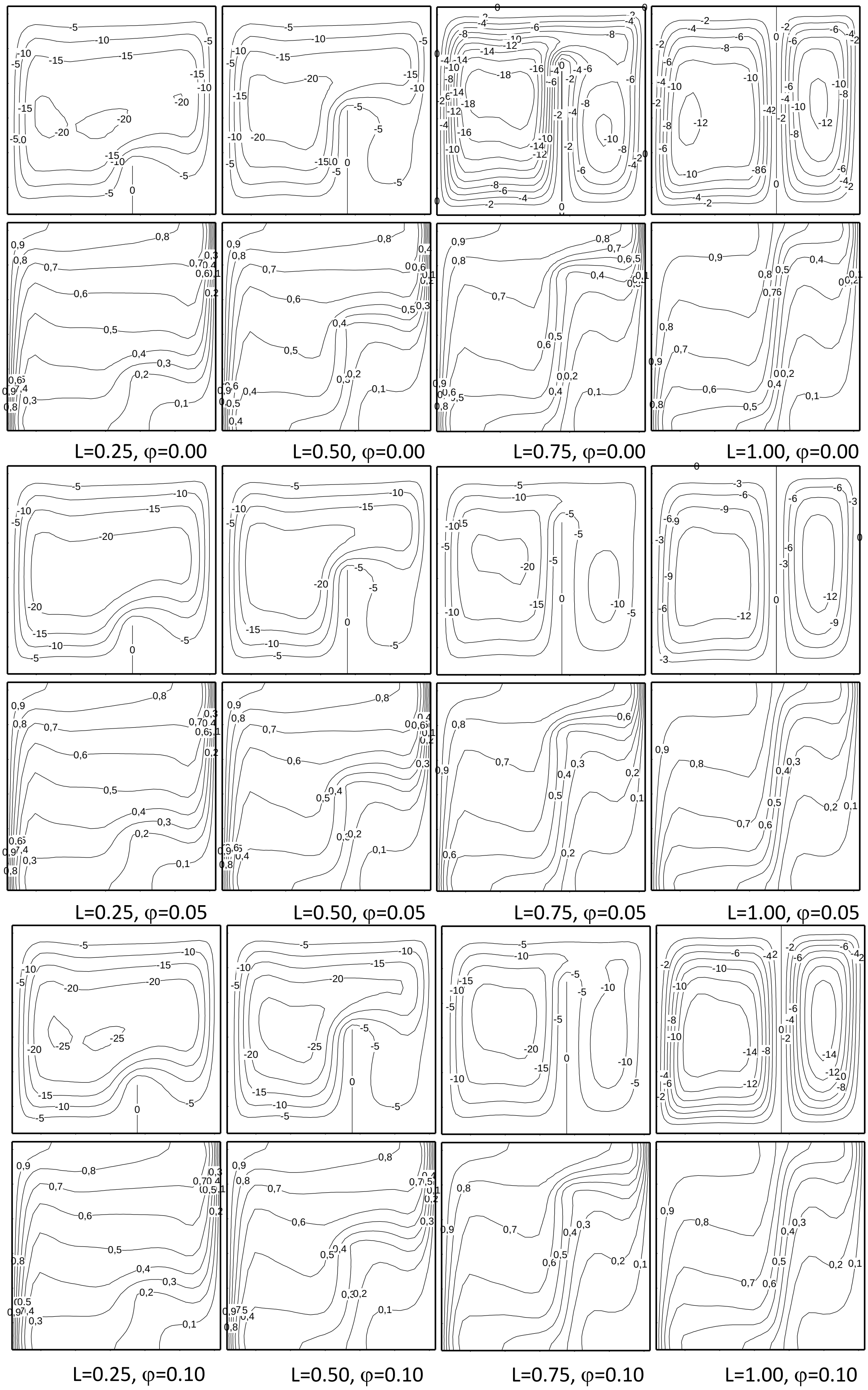

Figure 4. Streamlines and isotherms of copper based nanofluid for x_p=0.6 and Ra=10^6.

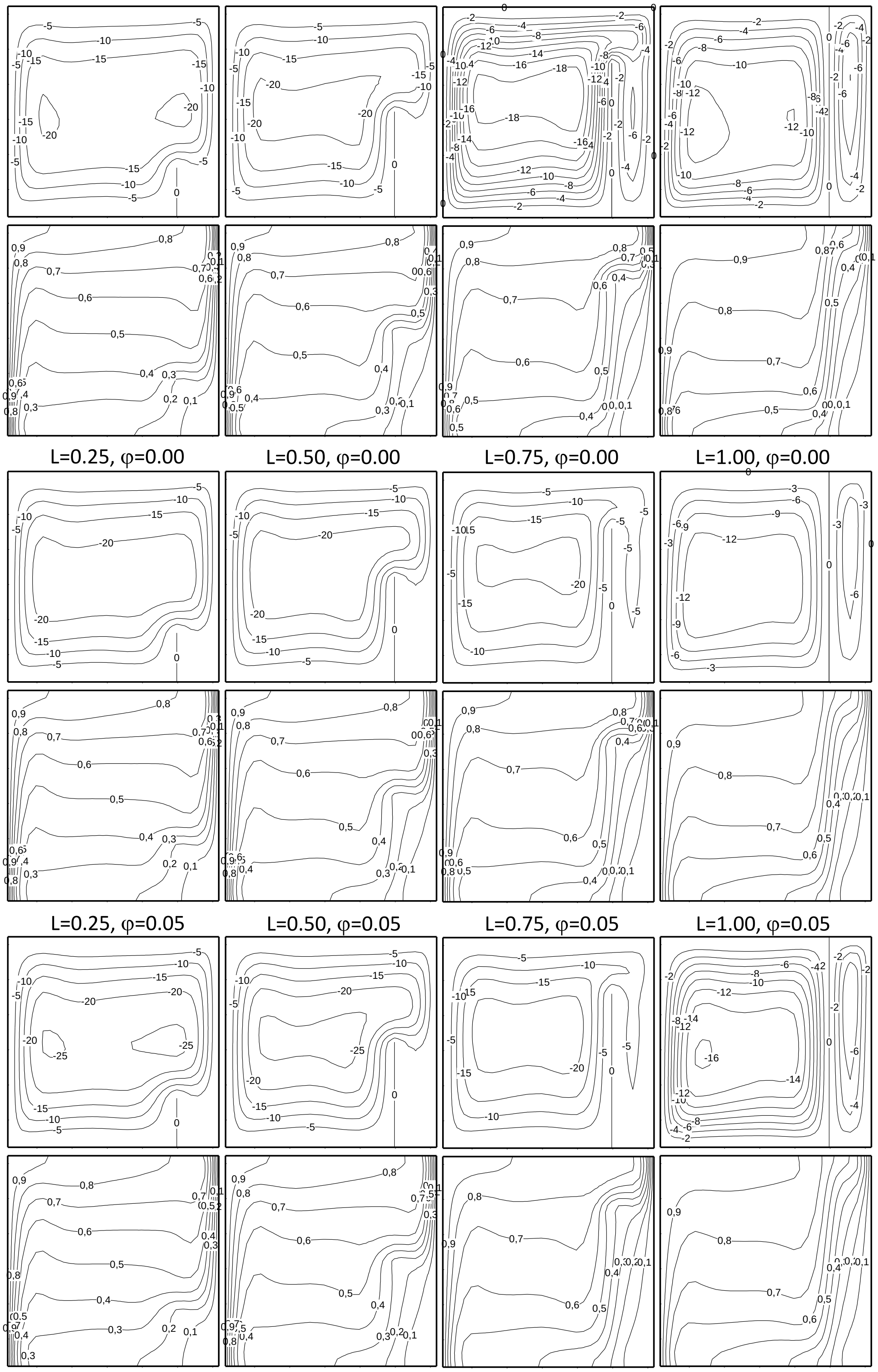

Figure 5. Streamlines and isotherms of copper based nanofluid for x_p=0.8 and Ra=10^6.

A series of grid systems of up to 31*31 points were performed to obtain a grid-independent mesh size, suggesting that when the mesh size is greater than 26x26, Nu_a on the hot wall and $|\psi|_{max}$ remain almost the same. Some results are shown in Table 2. Therefore a grid system of 31*31 was used in this study. The numbers of the mesh points used for the regions in the considered geometry are also listed in Table 3.

To validate the numerical code, the solution for the non-partitioned square enclosure with differentially heated sidewalls and adiabatic top and bottom walls were also computed and compared with the benchmark results of de Vahl Davis [32]. The results given in Table 4 showed that there was excellent agreement between the results of the numerical code used in the present study and the benchmark results of De Vahl Davis (De Vahl Davis, 1983).

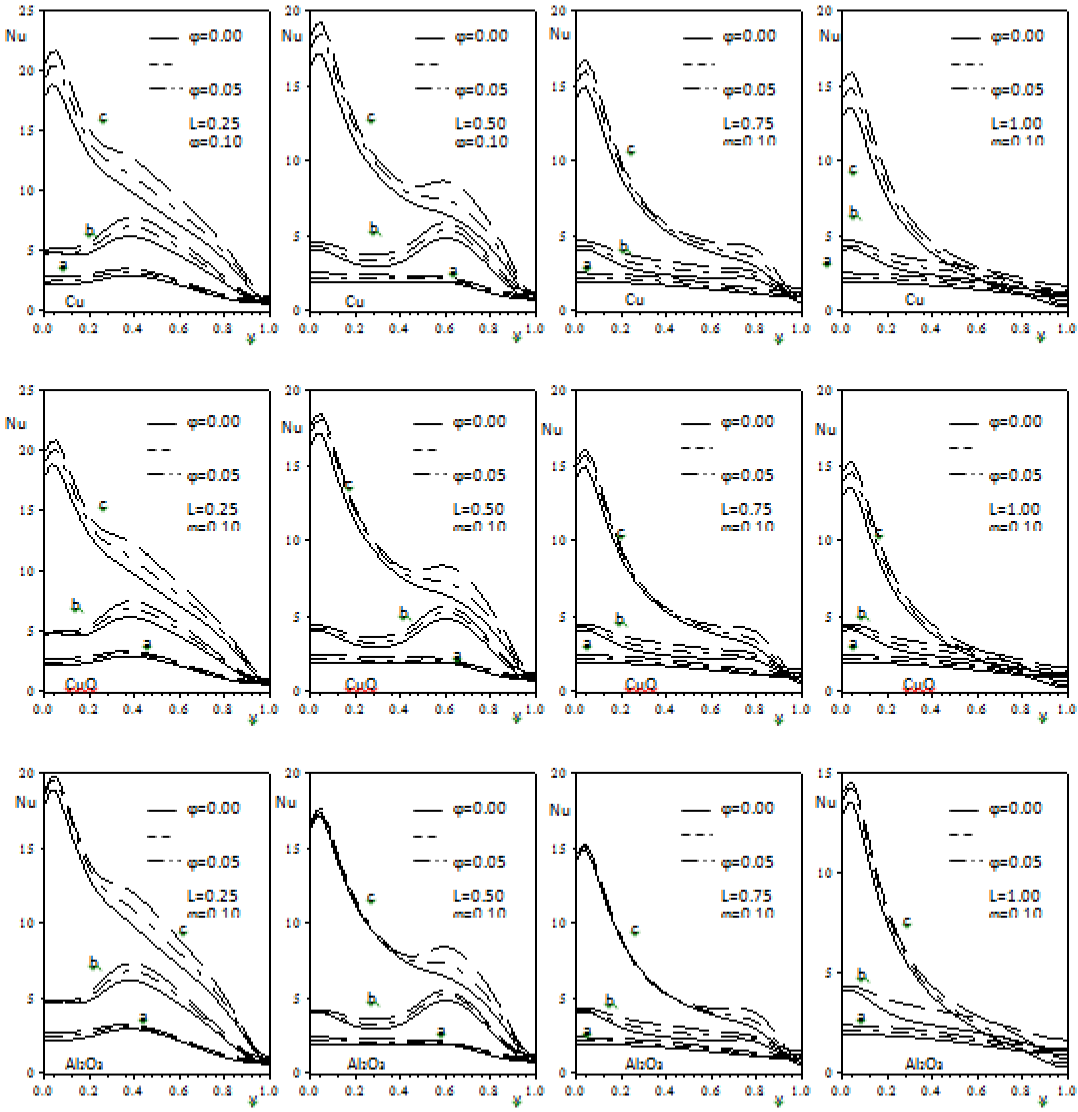

Figure 6. Local Nusselt number for x_p=0.2 and a) Ra=10^4, b) 10^5, c) Ra=10^6.

The streamlines and isotherms for various partition location values are shown in Figures 2-5 for CuO nanoparticle case. It can be seen that as the partition height increases, the circulation strength becomes weak as a result of increase in blocking effect of the partition on flow in the enclosure. Flow is single- cellular for low partition heights. Single cellular flow breaks down as partition height increases and a double cellular flow forms the flow field. When the partition divides the enclosure into two separate regions (l=1.0), single cellular flows constitutes the flow fields in both regions of the enclosure. Flows in these regions form as a consequence of the thermal interaction between these two regions. As expected, circulation strength in the smaller region is weaker for completely divided enclosure case because of higher viscous effects in this region. As can be seen from the figures that the circulation strength increases with increasing solid volume fraction as a result of higher energy transfer from the hot wall to the nanofluid with higher thermal conductivity. Furthermore, the isotherms become gradually parallel to the isothermal walls.

Variation of the local Nusselt number along the hot wall with the Rayleigh number, nanoparticle solid volume fraction, partition location and partition height can be seen in Figures 6- 8 for various nanofluids. As expected, the local Nusselt number is strongly dependent on the Rayleigh number and increases considerably with increasing Rayleigh numbers. When the partition is close to the hot wall, it obstructs the flow within the region between the hot wall and the partition, and relatively weak flow occurs in this region. Therefore, the local Nusselt number gets relatively lower values in this region. When this region is passed, local Nusselt number begins to take higher values. As the fluid particles moving along the hot wall are heated, the local Nusselt number begins to decrease again. When the partition is close to the hot wall, the Nusselt number displays two peak points. As apparent in the figures, the local Nusselt number gets lower values as the partition height increases because of its negative effect on the flow. As can be seen in the figures, the local Nusselt number exhibits a similar form for all nanofluids studied. The magnitude of the local Nusselt number differs for different types of nanofluids; it was higher for Cu nanoparticles. This is due to the higher thermal energy transport from the hot wall to the fluid with higher thermal conductivity. The figures also show the expected result that an increase in nanoparticle solid volume fraction leads to an increase in the local Nusselt number.

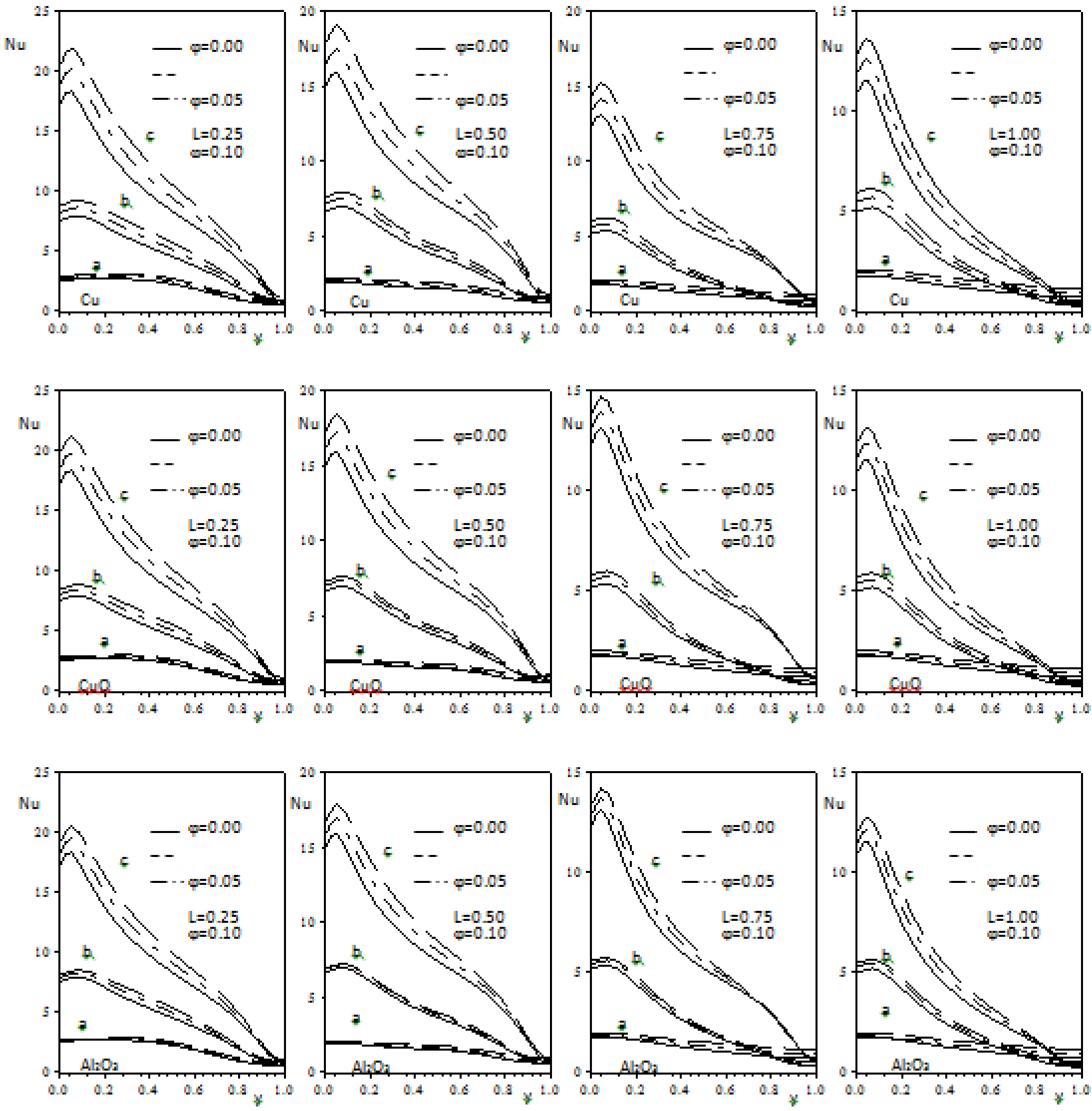

Figure 7. Local Nusselt number for x_p=0.4 and a) Ra=10^4, b) 10^5, c) Ra=10^6.

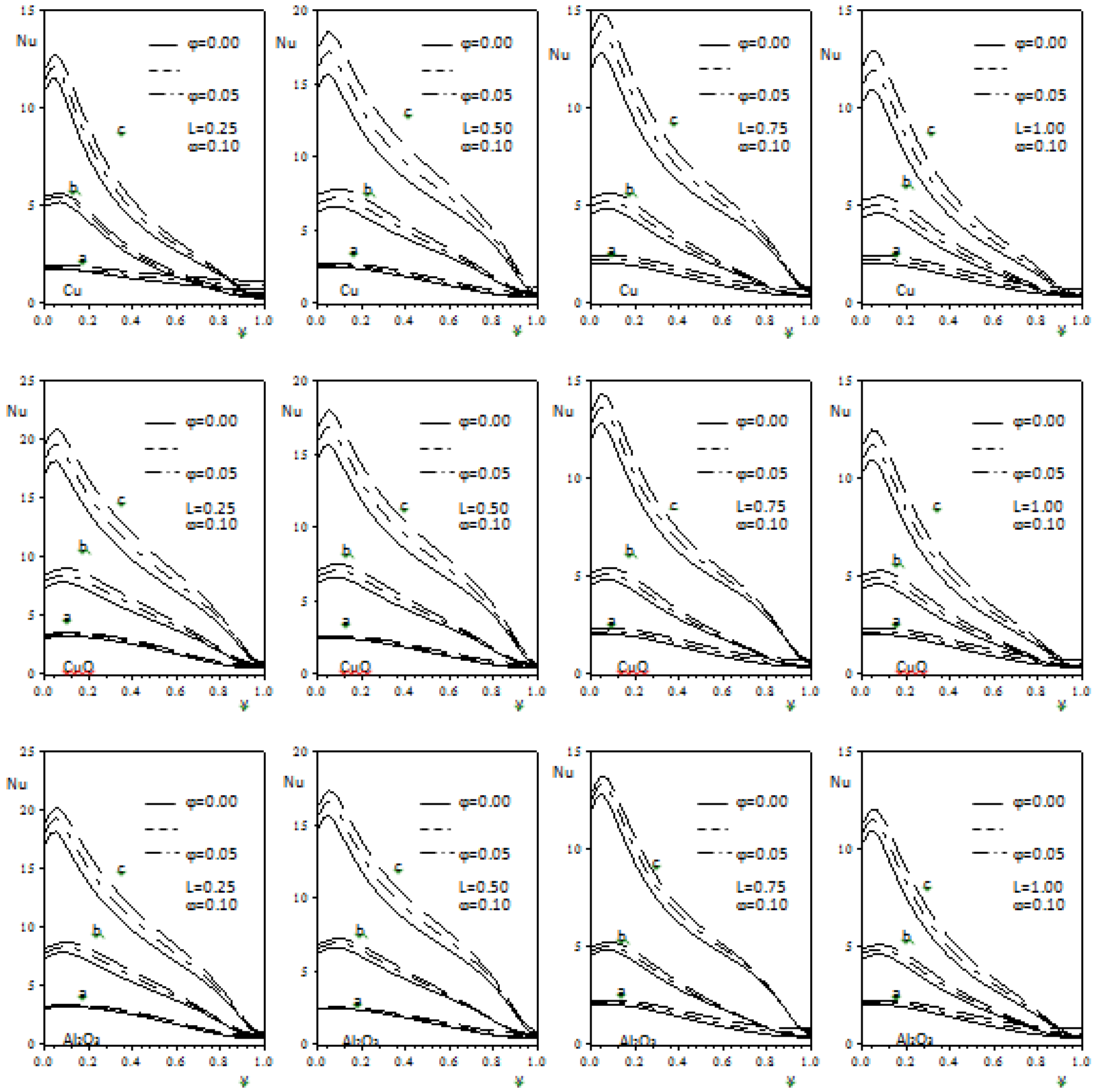

Figure 8. Local Nusselt number for x_p=0.6 and a) Ra=10^4, b) 10^5, c) Ra=10^6.

The variation of the average Nusselt number with various parameters considered in this study is shown in Tables 4-7. As stated above, circulation weakens with an increase in partition height and therefore, average Nusselt number takes lower values with increasing partition height. When the partition is close to the hot wall, it creates a negative effect on the flow in the smaller left region and prevents an effective heat transfer from the hot wall. When the partition is close to the cold wall, it creates a negative effect on the flow in the smaller right region and prevents an effective heat transfer from the cold wall, for high Rayleigh numbers. Consequently, as can be seen in the tables, the average Nusselt number initially increases and then decreases as the partition moves away from the hot wall and approaches to the cold wall. For low Rayleigh numbers, the Nusselt number initially decreases and then increases as the partition moves away from the hot wall because the partition has more effect on flow in the enclosure for these weak flow cases. As seen from the tables, the values of Nusselt number from the biggest to lowest are for Cu, CuO and Al_2O_3 nanoparticles. Increase in the average Nusselt number due to nanoparticle usage is up to 35% for Ra=10^4, up to 32% for Ra=10^5, and up to 25% for Ra=10^6. Furthermore, the average Nusselt number increases nearly linearly with increasing solid volume fraction.

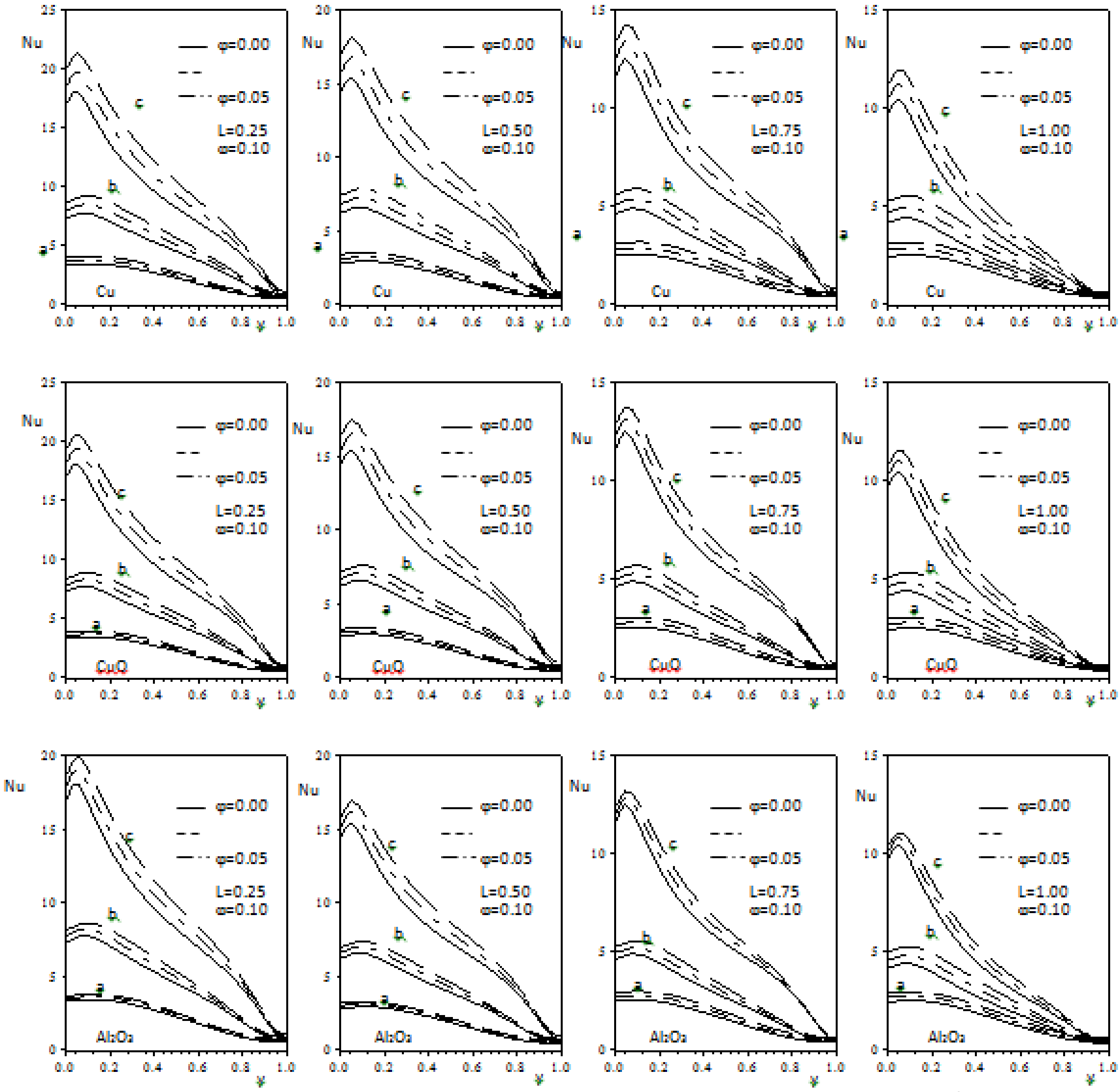

Figure 9. Local Nusselt number for x_p=0.8 and a) Ra=10^4, b) 10^5, c) Ra=10^6.

Table 4. Average Nusselt number for x_p=0.2.

			Cu		CuO		Al_2O_3	
l	Ra\j	0.00	0.05	0.10	0.05	0.10	0.05	0.10
0.25	10^4	2.01	2.24	2.47	2.20	2.38	2.17	2.31
	10^5	4.16	4.62	5.08	4.53	4.90	4.47	4.77
	10^6	8.84	9.86	10.85	9.67	10.46	9.54	10.16
0.50	10^4	1.66	1.87	2.09	1.84	2.02	1.82	1.98
	10^5	3.34	3.70	4.07	3.63	3.92	3.58	3.82
	10^6	7.74	8.52	9.22	8.35	8.88	8.21	8.56
0.75	10^4	1.53	1.75	1.98	1.72	1.91	1.71	1.883
	10^5	2.47	2.80	3.17	2.75	3.06	2.73	3.02
	10^6	5.79	6.26	6.69	6.13	6.43	6.00	6.15
1.00	10^4	1.53	1.75	1.98	1.72	1.91	1.70	1.88
	10^5	2.35	2.70	3.09	2.65	2.99	2.64	2.96
	10^6	4.34	4.84	5.34	4.74	5.14	4.68	5.01

Table 5. Average Nusselt number for x_p=0.4.

			Cu		CuO		Al_2O_3	
l	Ra\j	0.00	0.05	0.10	0.05	0.10	0.05	0.10
0.25	10^4	1.94	2.13	2.31	2.08	2.22	2.05	2.15
	10^5	4.49	4.98	5.45	4.88	5.25	4.81	5.08
	10^6	8.90	10.00	11.12	9.81	10.71	9.69	10.45
0.50	10^4	1.39	1.55	1.74	1.52	1.68	1.51	1.66
	10^5	3.78	4.12	4.41	4.03	4.24	3.95	4.04
	10^6	7.86	8.82	9.79	8.65	9.44	8.54	9.19
0.75	10^4	1.20	1.38	1.60	1.36	1.55	1.36	1.55
	10^5	2.46	2.68	2.91	2.63	2.80	2.58	2.70
	10^6	5.91	6.50	7.06	6.37	6.80	6.26	6.56
1.00	10^4	1.19	1.38	1.60	1.36	1.55	1.35	1.55
	10^5	2.27	2.53	2.79	2.48	2.69	2.45	2.62
	10^6	4.39	4.93	5.48	4.84	5.29	4.78	5.17

Table 6. Average Nusselt number for x_p=0.6.

			Cu		CuO		Al_2O_3	
l	Ra\j	0.00	0.05	0.10	0.05	0.10	0.05	0.10
0.25	10^4	2.03	2.22	2.41	2.18	2.32	2.14	2.24
	10^5	4.47	4.98	5.48	4.88	5.28	4.81	5.12
	10^6	8.88	9.96	11.06	9.77	10.67	9.66	10.40
0.50	10^4	1.50	1.64	1.81	1.61	1.74	1.58	1.70
	10^5	3.77	4.15	4.51	4.07	4.34	4.00	4.17
	10^6	7.82	8.77	9.71	8.60	9.36	8.49	9.11
0.75	10^4	1.20	1.39	1.60	1.36	1.55	1.36	1.55
	10^5	2.46	2.69	2.92	2.64	2.81	2.59	2.72
	10^6	5.99	6.59	7.16	6.47	6.89	6.36	6.65
1.00	10^4	1.19	1.38	1.60	1.36	1.55	1.35	1.55
	10^5	2.27	2.53	2.79	2.48	2.69	2.45	2.62
	10^6	4.40	4.94	5.49	4.85	5.30	4.79	5.17

Table 7. Average Nusselt number for x_p=0.8.

			Cu		CuO		Al_2O_3	
l	Ra\j	0.00	0.05	0.10	0.05	0.10	0.05	0.10
0.25	10^4	2.15	2.38	2.60	2.33	2.50	2.29	2.42
	10^5	4.44	4.95	5.46	4.86	5.27	4.80	5.13
	10^6	8.79	9.84	10.90	9.66	10.51	9.54	10.25
0.50	10^4	1.81	2.01	2.21	1.97	2.131	1.94	2.07
	10^5	3.82	4.26	4.69	4.18	4.52	4.12	4.39
	10^6	7.69	8.59	9.49	8.42	9.15	8.31	8.90
0.75	10^4	1.54	1.76	1.99	1.72	1.92	1.71	1.89
	10^5	2.69	3.01	3.35	2.95	3.23	2.92	3.16
	10^6	5.94	6.55	7.14	6.42	6.87	6.31	6.64
1.00	10^4	1.53	1.75	1.98	1.72	1.91	1.70	1.88
	10^5	2.34	2.70	3.09	2.65	2.99	2.64	2.96
	10^6	4.34	4.83	5.33	4.74	5.14	4.67	5.00

CONCLUSION

The natural convection heat transfer of water-based nanofluids in a differentially heated, partially divided enclosure was studied numerically for a range of partition locations, partition lengths, solid volume fractions and Rayleigh numbers. The results show that heat transfer decreases considerably with increasing partition height. Furthermore, as the distance of the partition from the hot wall increased, an initial decrease and a subsequent increase is observed in the average Nusselt number for low Rayleigh numbers and an initial increase and subsequent decrease is observed for high Rayleigh numbers. Heat transfer is considerably enhanced if the fluid contains nanoparticles. The highest increase in heat transfer occurs when Cu nanoparticles are used, and the lowest increase occurs when Al_2O_3 nanoparticles are used. Increase in the average Nusselt number due to nanoparticle usage is up to 35% for $Ra=10^4$, up to 32% for $Ra=10^5$ and up to 25% for $Ra=10^6$. The results also show that the average Nusselt number increases nearly linearly with solid volume

REFERENCES

Frederick, R. L. and Berbakow, O., Natural Convection in Cubical Enclosures with Thermal Sources on Adjacent Vertical Walls, *Numer. Heat Tr. A-Appl.* 41, 331-340, 2002.

Rahman, M. and Sharif, M. A. R., Numerical Study of Laminar Natural Convection in Inclined Rectangular Enclosures of Various Aspect Ratios, *Numer. Heat Tr. A-Appl.* 44(3), 355-373, 2003.

Kahveci, K., Numerical Simulation of Natural Convection in a Partitioned Enclosure Using PDQ Method, *Int. J. Numer. Meth. Heat Fluid Flow* 17(4), 439-456.

Kahveci, K., Natural Convection in a Partitioned Vertical Enclosure Heated with a Uniform Heat Flux, *ASME J. Heat Transfer* 129, 717-726.

Kahveci, K., A Differential Quadrature Solution of Natural Convection in an Enclosure with a Finite Thickness Partition, *Numer. Heat Tr. A-Appl.* 51(10), 979-1002, 2007.

Kahveci, K. and Öztuna, S., A Differential Quadrature Solution of MHD Natural Convection in an Inclined Enclosure with a Partition, *ASME J. Fluid Eng.* 130, 21102(14 pages), 2008.

Kahveci, K. and Oztuna, S., MHD Natural Convection Flow and Heat Transfer in a Laterally Heated Partitioned Enclosure, *European Journal of Mechanics B/Fluids* 28, 744-752, 2009.

Öztuna, S., A Differential Quadrature Solution of Natural Convection in an Enclosure with A Partial Partition, *Numer. Heat Tr. A-Appl.* 52(11), 1009-1026, 2007.

Eastman, J. A., Choi, S. U. S., Yu, W. and Thompson, L. J., Anomalously Increased Effective Thermal Conductivity of Ethylene Glycol-Based Nanofluids Containing Copper Nanoparticles, *Appl. Phys. Lett.* 78, 718-720, 2001.

Choi, S. U. S., Zhang, Z. G., Yu, W., Lockwood, F. E. and Grulke, E.A., Anomalous Thermal Conductivity Enhancement in Nanotube Suspension, *Appl. Phys. Lett.* 79, 2252-2254, 2001.

Xuan, Y. and Li, Q., 2000, Heat Transfer Enhancement of Nanofluids, *Int. J. Heat & Fluid Flow* 21, 158-164, 2000.

Keblinski, P., Phillpot, S. R., Choi, S. U. S. and Eastman, J. A., Mechanisms of Heat Flow in Suspensions of Nano-Sized Particles (Nanofluids), *Int. J. Heat Mass Tran.* 45, 855-863, 2002.

Eastman, J. A., Choi, S. U. S. , Li, S., Soyez, G, Thompson, L. J. and DiMelfi, R. J., Novel Thermal Properties of Nanostructured Materials, *J. Metastable Nanocryst. Mater.* 2, 629-637, 1998.

Wen, D. and Ding, Y., Experimental Investigation into Convective Heat Transfer of Nanofluids at the Entrance Region under Laminar Flow Conditions, *Int. J. Heat Mass Tran.* 47, 5181-5188, 2004.

Maiga, S. E. B., Nguyen, C. T., Galanis, N. and Roy, G., Heat Transfer Behaivours Of Nanofluids in a Uniformly Heated Tube, *Superlattice. Microst.* 35, 543-557, 2004.

Akbarinia, A. and Behzadmehr, A., Numerical Study of Laminar Mixed Convection of A Nanofluid in Horizontal Curved Tubes, *Appl. Therm. Eng.* 27(8-9), 1327-1337, 2007.

Izadi, M., Behzadmehr, A. and Jalali-Vahida, D., Numerical Study of Developing Laminar Forced Convection of a Nanofluid in an Annulus, *Int. J. Therm.Sci.* 48(11), 2119-2129, 2009.

Khanafer, K., Vafai, K. and Lightstone, M., Buoyancy Driven Heat Transfer Enhancement in a Two-Dimensional Enclosure Utilizing Nanofluids, *Int. J. Heat Mass Tran.* 46, 3639-3653, 2003.

Hwang, K. S., Lee, J.-H. and Jang, S.P., Buoyancy-Driven Heat Transfer of Water-Based Al_2O_3 Nanofluids in a Rectangular Cavity, *Int. J. Heat Mass Tran.* 50(19-20), 4003-4010, 2007.

Jou, R.-Y. and Tzeng, S.-C., Numerical Research of Nature Convective Hat Transfer Enhancement Filled with Nanofluids in Rectangular Enclosures, *Int. Commun. Heat Mass Transfer.* 33, 727-736, 2006.

Oztop, H. F. and Abu-Nada, E., Numerical Study of Natural Convection in Partially Heated Rectangular Enclosures Filled with Nanofluids, *Int. J. Heat Fluid Fl.* 29(5), 1326-1336, 2008.

Aminossadati, S. M. and Ghasemi B., Natural Convection Cooling of a Localised Heat Source at the Bottom of a Nanofluid-Filled Enclosure, *Eur. J. Mech. B-Fluid* 28(5), 630-640, 2009.

Tiwari, R. K. and Das, M. K., Heat Transfer Augmentation in a Two-Sided Lid-Driven Differentially Heated Square Cavity Utilizing Nanofluids, *Int. J. Heat Mass Tran.* 50, 2002-2018, 2007.

Kahveci, K., Buoyancy Driven Heat Transfer of Nanofluids in a Tilted Enclosure, *ASME J. Heat Transfer*, 132(6), 062501(12 pages), 2010.

Shu, C., Generalized Differential-Integral Quadrature and Application to the Simulation of Incompressible Viscous Flows Including Parallel Computation., *PhD thesis*, University of Glasgow, 1992.

Shu, C., *Differential Quadrature and its Application in Engineering*, Springer and Verlag, 2000.

Shu, C. and Richards, B. E., Application of Generalized Differential Quadrature to Solve Two–Dimensional Incompressible Navier Stokes Equations, *Int. J. Numer. Meth. Fluid*. 15, 791-798, 1992.

Belman, R. E., Kashef, B. G. and Casti, J., Differential Quadrature: A Technique for the Rapid Solution of Nonlinear Partial Differential Equations, *J. Comput. Phys.* 10, 40-52, 1972.

Yu, W. and Choi, S. U. S., The Role of Interfacial Layers in the Enhanced Thermal Conductivity of Nanofluids: A Renovated Maxwell Model, *J. Nanopart. Res.* 5, 167-171, 2003.

Brinkman, H. C., The Viscosity of Concentrated Suspensions and Solutions, *J. Chem. Phys.* 20, 571-581, 1952.

Xuan, Y. and Li, Q., Experimental Research on the Viscosity of Nanofluids, *Report of Nanjing University of Science and Technology*, in Chinese, 1999.

de Vahl Davis, G., Natural Convection of Air in a Square Cavity: A Benchmark Numerical Solution, *Int. J. Numer. Meth. Fluid.* 3, 249-264, 1983.

Semiha ÖZTUNA was born in Tekirdağ-Turkey in 1962. She graduated from the Mechanical Engineering Department of Trakya University in 1985. She obtained his MSc degree in 1990 and PhD degree in 1995 from Yıldız Technical University. She has been working as an Associate Professor at Trakya University since 2010. Her main research fields are heat transfer and fluid mechanics.

Kamil KAHVECİ was born in Bayburt-Turkey in 1971. He graduated from the Mechanical Engineering Department of Trakya University in 2003. He obtained his MSc degree in 1995 and PhD degree in 1998 from Trakya University. He has been working as an Associate Professor at Trakya University since 2010. His main research fields are heat transfer and fluid mechanics.